Quasi-two-dimensional behavior of phonon subsystems and the superconductivity mechanism in perovskitelike compounds

Yu. E. Kitaev, M. F. Limonov, and A. G. Panfilov
A. F. Ioffe Physical-Technical Institute, Politekhnicheskaya 26, 194021 St. Petersburg, Russia

R. A. Evarestov
St. Petersburg State University, Universit. pr. 2, Stary Peterhof, 198904 St. Petersburg, Russia

A. P. Mirgorodsky
Institute for Silicate Chemistry, Odoevskogo 24/2, 199155 St. Petersburg, Russia
(Received 10 May 1993; revised manuscript received 3 December 1993)

The results of group-theory analysis, lattice dynamical calculations, and experimental data on the vibrational spectra of perovskitelike superconductors have been considered together. The layer description of phonon subsystems in these materials has been shown to be valid. The quasi-two-dimensional nature of the phonon subsystems has been established. The genesis of the bulk modes has been studied. It has been shown that optical vibrations in these crystals can be divided into $3(N_L-1)$ interlayer and $3(N_A-N_L)$ intralayer modes where N_L and N_A are the numbers of layers and atoms per primitive unit cell, respectively. The interlayer bulk vibrations originate from acoustic layer modes whereas the intralayer modes are induced by optical vibrations of isolated layers. A sandwich conception of the high-T_c superconductivity mechanism is discussed based on the different roles of different layers.

I. INTRODUCTION

At the present stage of investigation of high-T_c superconductors, the most intriguing questions concern the common features of all perovskitelike-superconductor phonon spectra, and whether phonons are involved in the pairing mechanism for electrons. In this paper, we try to throw light on these problems.

The perovskitelike compounds have a pronounced layered structure. This gives rise to the quasi-two-dimensional (2D) behavior of the electron subsystem in these crystals. However, the question of the influence of the layered structure on the vibrational spectra remains open.

In Ref. 1, within the framework of the single-layer approach, a group-theory analysis of normal vibrations in Bi-based superconductors was performed. The crystal structure was artificially separated into individual layers and the layer mode symmetry was analyzed. However, unlike the case of the well-known layered crystals (As_2S_3, GaSe, etc.), the validity of such a separation is not obvious. Moreover, the choice of the division of the structure into individual layers is also ambiguous. In this paper, we verify the validity of the single-layer approach to the analysis of vibrational spectra of perovskitelike compounds by comparing the results of group-theory analysis with lattice dynamical calculations, and experimental data.

The paper is organized as follows. In Sec. II, the pronounced layered structure which is a general feature of perovskitelike superconductors is studied. All these compounds are built of a limited number of single layers. The layers are the common elements of the different superconducting compounds (Y, Bi, Tl based). This is used in Secs. III–VII in analyzing the symmetry of phonons, the vibrational spectra, and the role of phonons in the high-T_c superconductivity (HTSC) mechanism.

In the high-T_c superconductors under consideration, the number of atoms per primitive cell is relatively large. Hence, their vibrational spectra contain many lines whose assignment is rather complicated. However, the pronounced layered structure of these materials makes it possible to obtain additional information about lattice dynamics within the framework of symmetry considerations only.[1–4] Within such an approach, for La-, Y-, Bi-, and Tl-based superconductors, the symmetry of normal modes of isolated layers is analyzed; the layer vibrations are classified into acoustic and optical modes; and the bulk vibrations are classified into interlayer and intralayer modes (Sec. III). As a result, the symmetry correspondence between layer and bulk modes is established.

The results of lattice dynamical calculations for $YBa_2Cu_3O_7$ crystals are presented in Sec. IV. In these calculations the general valence-force-field model is used.

In Sec. V, we analyze the data obtained by Raman spectroscopy, which serves as a tool for obtaining information about lattice vibrations. A reliable interpretation of Raman-scattering spectra has been made for the $YBa_2Cu_3O_{7-\delta}$ superconductors.[5–7] To interpret with confidence the vibrational spectra of multi-component Bi-based superconductors, we carried out in Ref. 1 a comparative analysis of Raman spectra for a number of compounds formed by consecutive addition of new layers. As a consequence, it was established that the frequencies of Raman-active modes corresponding to the vibrations of atoms in certain layers varied insignificantly in different Bi-based compounds. That is to say, these

frequencies are the signatures of the layers. In this paper, we extend this conclusion to most principal superconductor families.

The main results of the group-theory analysis, the lattice dynamical calculations, and the analysis of general characteristics of the Raman spectra are summarized in Sec. VI. The conclusions of this section are used to analyze the "sandwich" model of high-T_c superconductivity, which is discussed in Sec. VII. Within this conception, the different layers are assumed to have different roles: the CuO_2 layers determine the electron-subsystem properties, and the separating layers induce high-frequency A_g phonons which determine $T_{c,\max}$ within each of the superconductor families.

II. LAYERED STRUCTURE OF HIGH-T_c SUPERCONDUCTORS

In this work, we analyze different high-T_c superconductors, namely those that are Y, Bi, and Tl based. To simplify comparison of vibrational spectra of different compounds, we propose an easy notation scheme (Fig. 1). It is based on the general layered structure of these materials. Since, in perovskitelike cuprates, each oxygen atom is in a certain metal-oxygen layer, this atom is labeled O, with a subscript denoting the metal atom in this layer. For example, the oxygen atom in the BiO layer is labeled O_{Bi} and that in the SrO layer is denoted as O_{Sr}.

The copper atoms belonging to double CuO_2 layers are labeled as Cu whereas those in single CuO_2 layers are denoted as Cu1 (Fig. 1). Similarly, the oxygen atoms in CuO_2 layers of tetragonal compounds are labeled O_{Cu} whereas the nonequivalent oxygen atoms O_{Cu} and O'_{Cu} in orthorhombic compounds are denoted by a prime. The oxygen atoms in the single layers are denoted as O_{Cu1}. For further analysis it is essential that the double CuO_2 layers are corrugated whereas the single CuO_2 layers are flat.

As an example of materials with layered architecture, let us consider Bi-based superconductors. The nonsuperconducting compounds without copper, $Bi_{1-x}(Sr_{1-y}Ca_y)_xO_{1.5-x/2}$,[1,8] could be chosen as parent structures of Bi superconductors. The other compounds of the Bi family can be built up by a consecutive insertion (layer by layer) of additional layers into the parent structure: $(Bi,Ca)O_\delta \rightarrow (Bi,Sr)O_\delta \rightarrow Bi_2Sr_2CuO_6 \rightarrow Bi_2Sr_2CaCu_2O_8 \rightarrow Bi_2Sr_2Ca_2Cu_3O_{10} \rightarrow Bi_4Sr_4CaCu_3O_{14}$. The systems most investigated are the $Bi_2Sr_2Ca_{n-1}Cu_nO_{2n+4}$ crystal family, including Bi-2:2:0:1 ($n=1$), Bi-2:2:1:2 ($n=2$), and Bi-2:2:2:3 ($n=3$) superconductors. Recently, $Bi_4Sr_4CaCu_3O_{14}$ (Bi-4:4:1:3) crystals were synthesized[9] and comprehensively studied.[10] The Bi-4:4:1:3 primitive cell is formed from halves of the Bi-2:2:0:1 and Bi-2:2:1:2 primitive cells.

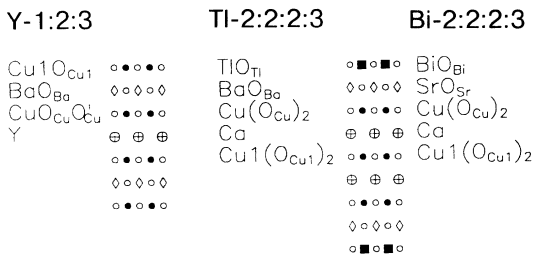

FIG. 1. Layer composition of crystal structures of high-T_c superconductors. The notations of the atoms are given alongside each layer.

The structures of Tl-based superconductors are also well known. Note the essential difference of Tl-based superconductors from the Bi-based ones: two Tl superconductor families with one or two TlO layers per unit cell are known at present. The formulas of these families are $TlBa_2Ca_{n-1}Cu_nO_{2n+3}$ and $Tl_2Ba_2Ca_{n-1}Cu_nO_{2n+4}$. The representatives of the first family are structurally similar to the 1:2:3 compounds, e.g., the $YBa_2Cu_3O_7$ and $CaBa_2TlCu_2O_7$ ($n=2$) crystals are isostructural. The second family is analogous to the $Bi_2Sr_2Ca_{n-1}Cu_nO_{2n+4}$ family, except that it is characterized by tetragonal symmetry with no evidence of the superstructure which is inherent in Bi-based superconductors.

The crystals of other HTSC families can be built up in a similar way. According to the block-layer concept,[11] the structure of cuprate superconductors can be viewed as a stack of conducting CuO_2 layers and different insulating ones (the block layers).

III. GROUP SYMMETRY ANALYSIS

In this section, the phonon symmetry of isolated layers is considered, the phonon symmetry of bulk crystals is analyzed, and finally the relationship between layer and bulk vibrational modes is established. For the complete group-theoretical analysis of both layer and bulk phonon symmetries, we use the method of induced band representations of space groups[4,12] which has proved to be much more efficient than the factor-group method,[13] especially for crystals with a large number of atoms per primitive cell and nonzero wave vectors $\mathbf{k}$ in the Brillouin zone (BZ).

A. Layer phonon symmetry

The layers are systems with 2D translational and 3D point symmetries. Therefore, the symmetry of a layer can be described by one of the 80 diperiodic groups (DG) in three dimensions. Each of these groups is a subgroup of one of the 230 triperiodic space groups G.[14]

In analyzing the crystal structures of perovskitelike compounds, we have divided them into a set of single layers and established the corresponding symmetries of isolated layers. The results are presented in Table I.

When determining the symmetry of isolated layers constituting the HTSC compounds under consideration, we take into account that the layer space group DG23 is a subgroup of the corresponding triperiodic group $G=C^1_{2v}(Pmm2)$, DG37 is a subgroup of $G=D^1_{2h}(P2/m2/m2/m)$, DG55 is a subgroup of $G=C^1_{4v}(P4mm)$, and DG61 is a subgroup of $G=D^1_{4h}(P4/mmm)$. Induced band representations of a diperiodic group DG can be obtained from induced band representations of a corresponding triperiodic space

TABLE I. Layer composition of perovskitelike superconductors, space symmetry groups (DG) of isolated layers, layer mode symmetries ($\Gamma_{ac}+\Gamma_{opt}$) and corresponding interlayer (Γ_{inter}) and intralayer (Γ_{intra}) bulk mode symmetries.

Layer	Symmetry of isolated layer	La_2CuO_4	Y 1:2:3	Number of layers Tl 1:2:0:1	Tl 1:1:1:2	Tl 1:2:2:3	Tl 2:2:0:1	Bi,Tl 2:2:1:2	Bi,Tl 2:2:2:3	Γ_{ac}	Γ_{opt}	Γ_{inter}	Γ_{intra}
$Cu(O_{Cu})_2$	$P2mm$(DG23)	2								$A_1+B_1+B_2$	$2(A_1+B_1+B_2)$	$A_g+B_{2g}+B_{3g}+B_{1u}+B_{2u}+B_{3u}$	$2(A_g+B_{1u})+2(B_{2g}+B_{3u})+2(B_{3g}+B_{2u})$
	$P4mm$(DG55)			2	2	2	2	2	2	A_1+E	A_1+B_1+2E	$A_{1g}+E_g+A_{2u}+E_u$	$(A_{1g}+A_{2u})+(B_{1g}+B_{2u})+2(E_g+E_u)$
	$P4/mmm$												
$Cu1(O_{Cu1})_2$	(DG61)	1	1		1	1		1		$A_{2u}+E_u$	$A_{2u}+B_{2u}+2E_u$	$A_{2u}+E_u$	$A_{2u}+B_{2u}+2E_u$
	$P2/m2/m2/m$												
$Cu1O_{Cu1}$	(DG37)		1							$B_{1u}+B_{2u}+B_{3u}$	$B_{1u}+B_{2u}+B_{3u}$	$B_{1u}+B_{2u}+B_{3u}$	$B_{1u}+B_{2u}+B_{3u}$
	$P2/m2/m2/m$												
Y	(DG37)		1							$B_{1u}+B_{2u}+B_{3u}$		$B_{1u}+B_{2u}+B_{3u}$	
	$P4/mmm$												
Ca	(DG61)				1	2		1	2	$A_{2u}+E_u$		$A_{2u}+E_u$	
BaO	$P2mm$(DG23)		2							$A_1+B_1+B_2$	$A_1+B_1+B_2$	$A_g+B_{2g}+B_{3g}+B_{1u}+B_{2u}+B_{3u}$	$(A_g+B_{1u})+(B_{2g}+B_{3u})+(B_{3g}+B_{2u})$
BaO, SrO,													
LaO	$P4mm$(DG55)	2		2	2	2	2	2	2	A_1+E	A_1+E	$A_{1g}+E_g+A_{2u}+E_u$	$(A_{1g}+A_{2u})+(E_g+E_u)$
T10,BiO	$P4mm$(DG55)						2	2	2	A_1+E	A_1+E	$A_{1g}+E_g+A_{2u}+E_u$	$(A_{1g}+A_{2u})+(E_g+E_u)$
	$P4/mmm$												
TlO	(DG61)			1	1	1				$A_{2u}+E_u$	$A_{2u}+E_u$	$A_{2u}+E_u$	$A_{2u}+E_u$

group G.[4]

In this paper, we discuss in detail the symmetry analysis procedure for the $YBa_2Cu_3O_7$ compound, whereas only final results are given for Bi- and Tl-based superconductors. The results of the group-theory analysis of phonon symmetry in the Y, BaO_{Ba}, $Cu1O_{Cu1}$, and $CuO_{Cu}O'_{Cu}$ layers constituting the $YBa_2Cu_3O_7$ compound are given in Tables II and III for the symmetry points of the primitive rectangular (2D) BZ.

Tables II and III have the following structure. Columns 1–3 contain the atomic arrangements over the Wyckoff positions (sites in direct space). Column 4 contains the Mulliken symbols of those irreducible representations (irreps) of the site symmetry groups for these Wyckoff positions, according to which the components of the vectors of local atomic displacements (x,y,z) transform. The remaining columns give the labels of induced representations in the **k** basis, with the symbols of **k** points (wave vectors) in the first row of the tables and the indices of small irreps of little groups in subsequent rows; these determine the symmetries of the normal modes. The labels of the layer group irreps correspond with those of the related triperiodic group G. In these tables and in all the following ones, the labeling of the space-group irreps is that of Ref. 15, the labeling of the point-group irreps is that of Ref. 16, and the site points **q** are indexed as Wyckoff positions from Ref. 17.

From Tables II and III, one can easily write down the full vibrational representation at any symmetry point of the BZ. For example, for the $Cu1O_{Cu1}$ layer, we obtain

$$\begin{aligned}\Gamma&=2\Gamma_2^-+2\Gamma_3^-+2\Gamma_4^-\ ,\\ X&=2X_2^-+2X_3^-+2X_4^-\ ,\\ Y&=Y_2^-+Y_3^-+Y_4^-+Y_1^++Y_2^++Y_3^+\ ,\\ S&=S_2^-+S_3^-+S_4^-+S_1^++S_2^++S_3^+\ .\end{aligned}\tag{1}$$

The corresponding vibrational representations at the BZ center for a complete set of layers for $YBa_2Cu_3O_7$ together with the results for Bi- and Tl-based compounds are presented in Table I. The layer modes at the BZ

TABLE II. Phonon symmetry in the $Cu1O_{Cu1}$ and Y layers. Primitive translations and site symmetry group for the direct lattice are $\mathbf{a}_1(1,0)$, $\mathbf{a}_2(0,1)$ (in units of ab) and $D_{2h}(mmm)$—$a(0,0,0)$, $e(0,\frac{1}{2},0)$, $f(\frac{1}{2},\frac{1}{2},0)$ (in units of $\mathbf{a}_i$); for the reciprocal lattice, $\mathbf{b}_1(1,0)$, $\mathbf{b}_2(0,1)$ (in units of $2\pi a,2\pi b$) and $D_{2h}(mmm)$—$\Gamma(0,0)$, $X(\frac{1}{2},0)$, $Y(0,\frac{1}{2})$, $S(\frac{1}{2},\frac{1}{2})$ (in units of $\mathbf{b}_i$).

$Cu1O_{Cu1}$	Y	$P2/m2/m2/m$(DG37)		Γ	X	Y	S
1	2	3	4	5	6	7	8
Cu1		1a	$b_{1u}(z)$	2^-	2^-	2^-	2^-
			$b_{2u}(y)$	4^-	4^-	4^-	4^-
			$b_{3u}(x)$	3^-	3^-	3^-	3^-
O_{Cu1}		1e	$b_{1u}(z)$	2^-	2^-	3^+	3^+
			$b_{2u}(y)$	4^-	4^-	1^+	1^+
			$b_{3u}(x)$	3^-	3^-	2^+	2^+
	Y	1f	$b_{1u}(z)$	2^-	4^+	3^+	1^-
			$b_{2u}(y)$	4^-	2^+	1^+	3^-
			$b_{3u}(x)$	3^-	1^+	2^+	4^-

TABLE III. Phonon symmetry in the $Cu(O_{Cu})_2$ and BaO layers. Primitive translations and site symmetry group for the direct lattice are $\mathbf{a}_1(1,0)$, $\mathbf{a}_2(0,1)$ (in units of *ab*) and $C_{2v}(2mm)$—$a(0,0,z)$, $b(0,\frac{1}{2},z)$, $c(\frac{1}{2},0,z)$, $d(\frac{1}{2},\frac{1}{2},0)$ (in units of $\mathbf{a}_i$); and for the reciprocal lattice, $\mathbf{b}_1(1,0)$, $\mathbf{b}_2(0,1)$ (in units of $2\pi/a, 2\pi/b$) and $C_{2v}(2mm)$—$\Gamma(0,0)$, $X(\frac{1}{2},0)$, $Y(0,\frac{1}{2})$, $S(\frac{1}{2},\frac{1}{2})$ (in units of $\mathbf{b}_i$).

$Cu(O_{Cu})_2$	BaO	$P2mm$(DG23)		Γ	*X*	*Y*	*S*
1	2	3	4	5	6	7	8
Cu	O_{Ba}	1*a*	$a_1(z)$	1	1	1	1
			$b_2(y)$	3	3	3	3
			$b_1(x)$	4	4	4	4
O_{Cu}	—	1*b*	$a_1(z)$	1	1	3	3
			$b_2(y)$	3	3	1	1
			$b_1(x)$	4	4	2	2
O'_{Cu}	—	1*c*	$a_1(z)$	1	4	1	4
			$b_2(y)$	3	2	3	2
			$b_1(x)$	4	1	4	1
—	Ba	1*d*	$a_1(z)$	1	4	3	2
			$b_2(y)$	3	2	1	4
			$b_1(x)$	4	1	2	3

center presented in Table I may be divided into "acoustic" and "optical" normal vibrations. Here and in future, we call the vibrations corresponding to a motion of a layer as an entity acoustic, and the others optical. It should be noted that monatomic layers (e.g., Y layers) give acoustic modes only. A layer with $N_i > 1$ nonequivalent atoms additionally gives $3(N_i - 1)$ optical modes.

Tables II and III also allow us to establish which atoms and local atomic displacements contribute to the modes with a given symmetry. This is especially important to interpret first- and second-order vibrational spectra. For example, one can see from Table II that at the *S* point of the BZ the mode with symmetry S_2^- is induced by *z* displacements of Cu1 atoms, whereas the mode with symmetry S_1^+ is induced by *y* displacements of O_{Cu1} atoms.

B. Bulk phonon symmetry

In a similar manner, we have obtained the phonon symmetry of the bulk $YBa_2Cu_3O_7$ crystals. The results are presented in Table IV. (The phonon symmetry over the entire BZ for Bi- and Tl-based crystals can be found elsewhere.[1,4,18–20])

From Table IV, one can easily write down the full vibrational representations at the symmetry points of the BZ. For example, at the Γ, *Z*, and *Y* points we have

$$\Gamma = 5\Gamma_1^+ + 5\Gamma_3^+ + 5\Gamma_4^+ + 8\Gamma_2^- + 8\Gamma_3^- + 8\Gamma_4^- ,$$
$$Y = 7Y_1^+ + 4Y_2^+ + 7Y_3^+ + 3Y_4^+ + 2Y_1^- + 6Y_2^- + 4Y_3^- + 6Y_4^- ,$$
$$Z = 7Z_1^+ + 7Z_3^+ + 7Z_4^+ + 6Z_2^- + 6Z_3^- + 6Z_4^- , \quad (2)$$

where, at the Γ point, the correspondence between two traditionally used sets of notations is the following: $\Gamma_1^+ = A_g$, $\Gamma_3^+ = B_{3g}$, $\Gamma_4^+ = B_{2g}$, $\Gamma_2^- = B_{1u}$, $\Gamma_3^- = B_{3u}$, and $\Gamma_4^- = B_{2u}$.

C. The correspondence between layer and bulk modes

We now establish the correspondence between layer and bulk modes. Since, for the $YBa_2Cu_3O_7$ lattice, the

TABLE IV. Phonon symmetry in $YBa_2Cu_3O_7$ compounds. Primitive translations and site symmetry groups for the direct lattice are $\mathbf{a}_1(1,0,0)$, $\mathbf{a}_2(0,1,0)$, $\mathbf{a}_3(0,0,1)$ (in units of *abc*) and $D_{2h}(mmm)$—$c(0,0,\frac{1}{2})$, $f(\frac{1}{2},\frac{1}{2},0)$, $g(0,\frac{1}{2},\frac{1}{2})$; $C_{2v}(2mm)$—$q(0,0,z)$, $r(0,\frac{1}{2},z)$, $s(\frac{1}{2},0,z)$, $t(\frac{1}{2},\frac{1}{2},z)$ (in units of $\mathbf{a}_i$); and for the reciprocal lattice, $\mathbf{b}_1(1,0,0)$, $\mathbf{b}_2(0,1,0)$, $\mathbf{b}_3(0,0,1)$ (in units of $\mathbf{b}_i$) and $D_{2h}(mmm)$—$\Gamma(0,0,0)$, $X(\frac{1}{2},0,0)$, $Y(0,\frac{1}{2},0)$, $Z(0,0,\frac{1}{2})$, $S(\frac{1}{2},\frac{1}{2},0)$, $T(0,\frac{1}{2},\frac{1}{2})$, $U(\frac{1}{2},0,\frac{1}{2})$, $R(\frac{1}{2},\frac{1}{2},\frac{1}{2})$ (in units of $\mathbf{b}_i$).

$D_{2h}^1(Pmmm)$			Γ	*X*	*Y*	*Z*	*S*	*T*	*U*	*R*
Cu1	1*c*	$b_{1u}(z)$	2^-	2^-	2^-	1^+	2^-	1^+	1^+	1^+
		$b_{2u}(y)$	4^-	4^-	4^-	3^+	4^-	3^+	3^+	3^+
		$b_{3u}(x)$	3^-	3^-	3^-	4^+	3^-	4^+	4^+	4^+
Y	1*f*	$b_{1u}(z)$	2^-	4^+	3^+	2^-	1^-	3^+	4^+	1^-
		$b_{2u}(y)$	4^-	2^+	1^+	4^-	3^-	1^+	2^+	3^-
		$b_{3u}(x)$	3^-	1^+	2^+	3^-	4^-	2^+	1^+	4^-
O_{Cu1}	1*g*	$b_{1u}(z)$	2^-	2^-	3^+	1^+	3^+	4^-	1^+	4^-
		$b_{2u}(y)$	4^-	4^-	1^+	3^+	1^+	2^-	3^+	2^-
		$b_{3u}(x)$	3^-	3^-	2^+	4^+	2^+	1^-	4^+	1^-
O_{Ba}	2*q*	$a_1(z)$	$1^+,2^-$	$1^+,2^-$	$1^+,2^-$	$1^+,2^-$	$1^+,2^-$	$1^+,2^-$	$1^+,2^-$	$1^+,2^-$
Cu		$b_1(x)$	$3^-,4^+$	$3^-,4^+$	$3^-,4^+$	$3^-,4^+$	$3^-,4^+$	$3^-,4^+$	$3^-,4^+$	$3^-,4^+$
		$b_2(y)$	$3^+,4^-$	$3^+,4^-$	$3^+,4^-$	$3^+,4^-$	$3^+,4^-$	$3^+,4^-$	$3^+,4^-$	$3^+,4^-$
O_{Cu}	2*r*	$a_1(z)$	$1^+,2^-$	$1^+,2^-$	$3^+,4^-$	$1^+,2^-$	$3^+,4^-$	$3^+,4^-$	$1^+,2^-$	$3^+,4^-$
		$b_1(x)$	$3^-,4^+$	$3^-,4^+$	$1^-,2^+$	$3^-,4^+$	$1^-,2^+$	$1^-,2^+$	$3^-,4^+$	$1^-,2^+$
		$b_2(y)$	$3^+,4^-$	$3^+,4^-$	$1^+,2^-$	$3^+,4^-$	$1^+,2^-$	$1^+,2^-$	$3^+,4^-$	$1^+,2^-$
O'_{Cu}	2*s*	$a_1(z)$	$1^+,2^-$	$3^-,4^+$	$1^+,2^-$	$1^+,2^-$	$3^-,4^+$	$1^+,2^-$	$3^-,4^+$	$3^-,4^+$
		$b_1(x)$	$3^-,4^+$	$1^+,2^-$	$3^-,4^+$	$3^-,4^+$	$1^+,2^-$	$3^-,4^+$	$1^+,2^-$	$1^+,2^-$
		$b_2(y)$	$3^+,4^-$	$1^-,2^+$	$3^+,4^-$	$3^+,4^-$	$1^-,2^+$	$3^+,4^-$	$1^-,2^+$	$1^-,2^+$
Ba	2*t*	$a_1(z)$	$1^+,2^-$	$3^-,4^+$	$3^+,4^-$	$1^+,2^-$	$1^-,2^+$	$3^+,4^-$	$3^-,4^+$	$1^-,2^+$
		$b_1(x)$	$3^-,4^+$	$1^+,2^-$	$1^-,2^+$	$3^-,4^+$	$3^+,4^-$	$1^-,2^+$	$1^+,2^-$	$3^+,4^-$
		$b_2(y)$	$3^+,4^-$	$1^-,2^+$	$1^+,2^-$	$3^+,4^-$	$3^-,4^+$	$1^+,2^-$	$1^-,2^+$	$3^-,4^+$

layer groups DG23 and DG37 are subgroups of the space group of the bulk crystal (D_{2h}^1), the mode correspondence can be obtained by the direct induction procedure.[4]

For the Y layer, the layer modes transform into the following bulk modes

$$\Gamma_2^- \rightarrow \Gamma_2^- + Z_2^- ; \quad \Gamma_3^- \rightarrow \Gamma_3^- + Z_3^- ; \quad \Gamma_4^- \rightarrow \Gamma_4^- + Z_4^- , \tag{3}$$

whereas those of the $Cu1O_{Cu1}$ layer transform into

$$\Gamma_2^- \rightarrow \Gamma_2^- + Z_1^+ ; \quad \Gamma_3^- \rightarrow \Gamma_3^- + Z_4^+ ; \quad \Gamma_4^- \rightarrow \Gamma_4^- + Z_3^+ . \tag{4}$$

The layer vibrations of $Cu(O_{Cu})_2$ and BaO layers transform into the following bulk modes

$$\begin{aligned} &\Gamma_1 \rightarrow \Gamma_1^+ + \Gamma_2^- + Z_1^+ + Z_2^- ; \\ &\Gamma_3 \rightarrow \Gamma_3^+ + \Gamma_4^- + Z_3^+ + Z_4^- ; \\ &\Gamma_4 \rightarrow \Gamma_4^+ + \Gamma_3^- + Z_4^+ + Z_3^- . \end{aligned} \tag{5}$$

Taking into account that the perovskitelike crystals have pronounced layered structures and supposing that intralayer interactions are stronger than interlayer ones, it is natural to assume that the normal-mode spectra consist of intralayer and interlayer vibrations. The latter are superpositions of displacements of different layers relative to each other.

Since acoustic layer modes at the BZ center correspond to the translations of a layer as a whole, they transform into interlayer bulk modes. The optical layer modes transform into intralayer bulk modes.

Thus, for the Y layer, the general relationship between layer (Γ_L) and bulk crystals (Γ_C) modes is the following

$$\begin{aligned} \Gamma_L &= \Gamma_{ac} + \Gamma_{opt} = (B_{1u} + B_{2u} + B_{3u}) + (O) \\ &\rightarrow \Gamma_C = \Gamma_{inter} + \Gamma_{intra} \\ &= (B_{1u} + B_{2u} + B_{3u}) + (O) , \end{aligned} \tag{6}$$

whereas for the $Cu1O_{Cu1}$ layer we have

$$\begin{aligned} \Gamma_L &= \Gamma_{ac} + \Gamma_{opt} \\ &= (B_{1u} + B_{2u} + B_{3u}) + (B_{1u} + B_{2u} + B_{3u}) \\ &\rightarrow \Gamma_C = \Gamma_{inter} + \Gamma_{intra} \\ &= (B_{1u} + B_{2u} + B_{3u}) + (B_{1u} + B_{2u} + B_{3u}) . \end{aligned} \tag{7}$$

Similarly, for the $Cu(O_{Cu})_2$ layer, the mode relationship is

$$\begin{aligned} \Gamma_L &= \Gamma_{ac} + \Gamma_{opt} = (A_1 + B_1 + B_2) + (2A_1 + 2B_1 + 2B_2) \\ &\rightarrow \Gamma_C = \Gamma_{inter} + \Gamma_{intra} = (A_g + B_{1u} + B_{2g} + B_{3u} + B_{3g} + B_{2u}) + 2(A_g + B_{1u} + B_{2g} + B_{3u} + B_{3g} + B_{2u}) , \end{aligned} \tag{8}$$

whereas that for the BaO_{Ba} layer is

$$\begin{aligned} \Gamma_L &= \Gamma_{ac} + \Gamma_{opt} = (A_1 + B_1 + B_2) + (A_1 + B_1 + B_2) \\ &\rightarrow \Gamma_C = \Gamma_{inter} + \Gamma_{intra} = (A_g + B_{1u} + B_{2g} + B_{3u} + B_{3g} + B_{2u}) + (A_g + B_{1u} + B_{2g} + B_{3u} + B_{3g} + B_{2u}) . \end{aligned} \tag{9}$$

Summing the contributions of the layers, we obtain the result that, for the $YBa_2Cu_3O_7$ crystal, the full vibrational representation at the Γ point of the BZ can be divided into acoustic, interlayer, and intralayer optical modes as follows:

$$\begin{aligned} \Gamma_C = \Gamma_{ac} + \Gamma_{inter} + \Gamma_{intra} &= (B_{1u} + B_{2u} + B_{3u}) + (2A_g + 3B_{1u} + 2B_{2g} + 3B_{3u} + 2B_{3g} + 3B_{2u}) \\ &\quad + (3A_g + 4B_{1u} + 3B_{2g} + 4B_{3u} + 3B_{3g} + 4B_{2u}) . \end{aligned} \tag{10}$$

(Similar results for a complete set of layers in La-, Bi-, and Tl- based compounds are listed in Table I.)

So, the main results of the group-theory analysis are as follows.

(i) In $YBa_2Cu_3O_7$, the bulk modes can be classified into three acoustic modes, 15 interlayer modes (originating from layer acoustic vibrations), and 21 intralayer modes (originating from layer optical vibrations). It is easy to obtain the general case that the number of interlayer modes is equal to $3(N_L - 1)$, where N_L is the number of layers per unit cell in the layered compounds under consideration. The number of intralayer modes is equal to $3(N_A - N_L)$ with N_A being the total number of atoms per unit cell.

Thus, the vibrational representation at the Γ point of the BZ can be written in any one of the layered crystals as follows,

$$\Gamma = 3\Gamma_{ac} + 3(N_L - 1)\Gamma_{inter} + 3(N_A - N_L)\Gamma_{intra} . \tag{11}$$

(ii) It follows from Eq. (5) that, for a weak interlayer interaction, there is a small frequency splitting of intralayer modes. In this case, the frequencies of the intralayer bulk phonons with symmetries Γ_1^+ (A_g) and Γ_2^- (B_{1u}) as well as Γ_3^+ (B_{3g}) and Γ_4^- (B_{2u}) or Γ_4^+ (B_{2g}) and Γ_3^- (B_{3u}) modes should be close. Since the space group of $Cu(O_{Cu})_2$ and BaO_{Ba} layers does not contain an inversion, the layer modes Γ_1 (A_1), Γ_3 (B_2), and Γ_4 (B_1) are both ir and Raman active. At the same time, the space group of the bulk crystal contains an inversion. Therefore, in the corresponding Davydov doublets originating from the layer optical modes, the even components Γ_1^+ (A_g), Γ_3^+ (B_{3g}), and Γ_4^+ (B_{2g}) are Raman active whereas the odd components Γ_2^- (B_{1u}), Γ_4^- (B_{2u}) and Γ_3^- (B_{3u}) are infrared active. It should be stressed that the magnitudes

of the splittings are determined by the interlayer interaction. Thus, the intralayer modes of noncentrosymmetrical layers induce Davydov doublets in centrosymmetrical bulk crystals. In $YBa_2Cu_3O_7$, there are three (A_g,B_{1u}), three (B_{3g},B_{2u}), and three (B_{2g},B_{3u}) doublets.

(iii) One can also see from Eqs. (4), (5) that the frequencies of the corresponding intralayer bulk modes at the Γ and Z points should be close. In other words, the intralayer modes are almost dispersionless along the Γ-Z symmetry line. This correlates with the results of theory[21] and has been proved to be correct by neutron-scattering experiments. It will be discussed below.

IV. DYNAMICAL CALCULATIONS

To comprehend better the properties of phonon subsystems of high-T_c superconductors, we have performed a lattice dynamical treatment of the $YBa_2Cu_3O_7$ lattice within a unified description of its potential function. The results of similar computations of $YBa_2Cu_3O_6$ and $GdBa_2Cu_3O_7$ will be presented in detail elsewhere.[22]

We used the general valence-force-field model (GVFF), program code CRYME,[23] and the structural data determined at ambient conditions in Ref. 24. The force-constant magnitudes have been derived from a fitting procedure using the experimentally measured frequencies of ir- and Raman-active modes,[5–7,25] and the linear compressibilities given in Ref. 26. The set of GVFF parameters adopted (see Table V) consists of diagonal stretching constants S_1–S_{12}, diagonal bending constants B_1–B_3, and two off-diagonal constants H_1,H_2 describing stretch-stretch interactions. The H_2 constant has been found to be of extreme importance in reproducing some of the principal peculiarities of the properties considered.[22]

TABLE V. Force constants for $YBa_2Cu_3O_7$.

	Atoms involved	Distance (Å) or angle (deg)	Value[a]
S_1	Cu1-O_{Ba}	1.837	1.8
S_2	Cu-O_{Cu}	1.931	1.35
S_3	Cu1-O_{Cu1}	1.943	1.3
S_4	Cu-O'_{Cu}	1.961	1.25
S_5	Cu-O_{Ba}	2.315	0.7
S_6	Y-O'_{Cu}	2.384	0.55
	Y-O_{Cu}	2.400	0.55
S_7	Ba-O_{Ba}	2.743	0.27
S_8	Ba-O_{Cu1}	2.880	0.23
S_9	Ba-O'_{Cu}	2.960	0.2
	Ba-O_{Cu}	2.996	0.2
S_{10}	O_{Cu}-O_{Cu}	2.817	0.2
	O'_{Cu}-O'_{Cu}	2.854	0.2
S_{11}	Ba-Cu1	3.474	0.2
S_{12}	Y-Cu	3.207	0.1
B_1	O_{Cu}-Cu-O'_{Cu}	88.87	0.45
B_2	O_{Ba}-Cu1-O_{Cu1}	90.00	0.45
B_3	O_{Ba}-Cu-O'_{Cu}	97.74	0.15
	O_{Ba}-Cu-O_{Cu}	98.42	0.15
H_1	O_{Ba}-Cu1, Cu1-O_{Ba}		−0.2
H_2	O_{Cu}-Y, Y-O_{Cu}		0.13

[a]Force constant units are: S_i, mdyn/Å; B_i, mdyn Å; and H_i, mdyn/Å.

The above force constants lead to the set of optical frequencies given in Table VI for the BZ center $\Gamma(0,0,0)$ and for the symmetry points $Z(0,0,\pi/c)$ and $Y(0,\pi/b,0)$. The calculated displacement patterns corresponding to each of these modes in the BZ center are also presented in Table VI. When analyzing this table, one can come to some important conclusions, which we discuss below.

A. Interlayer modes

Let us scrutinize the low-frequency vibrations. These modes are usually attributed to the heavy-metal-atom vibrations, each of the vibrations being connected with atoms of a certain kind. However, according to our computations, another approach is more correct. It can be seen from Table VI that most of the low-frequency modes are formed by displacements of certain layers relative to each other. What is more, for different atoms in one layer, displacement amplitudes are close in some cases. So, the displacement patterns resemble translations of layers as a whole. These modes can be regarded as interlayer vibrations.

In particular, low-frequency vibrations of B_{2g} and B_{3g} symmetries appear to be in-phase (with frequencies 78 and 79 cm^{-1}) and out-of-phase (103 and 104 cm^{-1}) displacements of the BaO_{Ba} and $CuO_{Cu}O'_{Cu}$ layers relative to immobile $Cu1O_{Cu1}$ and Y layers. By the way, Y, Cu1, and O_{Cu1} atoms do not participate in even vibrations at all.

Unlike B_{2g} and B_{3g} modes, the interlayer character of low-frequency A_g modes does not manifest itself so strongly. The amplitudes of z displacements of Ba (110 cm^{-1}) and Cu (151 cm^{-1}) atoms are larger than those of oxygen atoms.

In the case of odd vibrations of low frequency, all four layers are displaced. For instance, the out-of-phase shift of the Y and $CuO_{Cu}O'_{Cu}$ layers relative to the BaO_{Ba} and $Cu1O_{Cu1}$ layers corresponds to the 64-cm^{-1} vibration of the B_{3u} symmetry.

Thus, the number of modes which could be attributed to interlayer ones according to lattice dynamical calculations is 15. These are low-frequency modes $(2A_g+3B_{1u}+2B_{2g}+3B_{3u}+2B_{3g}+3B_{2u})$—see Table VI. Hence, the results obtained by lattice dynamical calculations agree with those of the group-theory analysis.

B. Intralayer modes

Quite different is the case of higher-frequency vibrations. It is seen from Table VI that each of these modes is formed by the displacements of oxygen atoms belonging to one layer. The other atoms are displaced an order of magnitude less. Therefore, these modes can be attributed to intralayer vibrations, with each mode being induced by an optical vibration of an isolated layer. From Table VI, it follows that there are 21 high-frequency intralayer vibrations, namely $(3A_g+4B_{1u}+3B_{2g}+4B_{3u}+3B_{3g}+4B_{2u})$, which coincides with the results of symmetry analysis.

Let us consider three high-frequency A_g modes. The 335-cm^{-1} vibration originates from out-of-phase displacements along the z axis of atoms O_{Cu} and O'_{Cu}; the 439-cm^{-1} vibration is formed on the whole by in-phase z displacements of the same atoms; the 502-cm^{-1} vibration is determined by z displacements of the O_{Ba} atoms.

C. The splitting of layer vibrations

The above symmetry analysis predicts that every layer mode should split into two vibrations when passing from an isolated layer without an inversion center (CuO_2 and BaO in $YBa_2Cu_3O_7$) to the bulk centrisymmetrical crystal. One of the vibrations should be Raman active and its counterpart ir active. For layers with an inversion center, each layer mode transforms into one bulk mode.

The model computations confirm this. It is seen from Table VI that every high-frequency (intralayer) even vibration of atoms belonging to $Cu(O_{Cu})_2$ and BaO_{Ba} layers has as a counterpart a corresponding odd vibration with similar displacements of atoms. At the same time, the vibrations of atoms located in $Cu1O_{Cu1}$ and Y layers do not give such doublets. Note, the frequencies of components differ slightly both within the three doublets (B_{2g},B_{3u})

TABLE VI. Calculated frequencies at the Γ, Z, and Y symmetry points and displacements of atoms at the Γ point in $YBa_2Cu_3O_7$. The amplitudes of atomic displacements are given within an accuracy of 0.5 a.u.; the atomic displacements with amplitudes less than 0.5 a.u. are not presented. The displacements of atoms of the upper half of the primitive unit cell are given. The corresponding atoms of the lower part move in phase for odd modes and out of phase for even modes.

Γ	Z	Y	Atomic displacements at the Γ point of the BZ
			A_g
110	74	123	$6^Z\mathrm{Ba}+(1^Z\mathrm{Cu}+1^Z\mathrm{O_{Cu}}+1^Z\mathrm{O'_{Cu}})$
151	164	164	$3^Z\mathrm{O_{Ba}}+(9^Z\mathrm{Cu}+1^Z\mathrm{O_{Cu}}+1^Z\mathrm{O'_{Cu}})$
335	335	343	$13^Z\mathrm{O_{Cu}}-12^Z\mathrm{O'_{Cu}}$
439	439	496	$12^Z\mathrm{O_{Cu}}+13^Z\mathrm{O'_{Cu}}-1^Z\mathrm{Cu}-1^Z\mathrm{O_{Ba}}$
502	502	501	$17^Z\mathrm{O_{Ba}}-1^Z\mathrm{Cu}$
			B_{2g}
78	90	116	$(5^X\mathrm{Ba}+5^X\mathrm{O_{Ba}})+(4^X\mathrm{Cu}+4^X\mathrm{O_{Cu}}+2^X\mathrm{O'_{Cu}})$
103	99	117	$(3^X\mathrm{Ba}+2^X\mathrm{O_{Ba}})-(7^X\mathrm{Cu}+7^X\mathrm{O_{Cu}}+3^X\mathrm{O'_{Cu}})$
261	261	248	$17^X\mathrm{O_{Ba}}-2^X\mathrm{Ba}-1^X\mathrm{O'_{Cu}}$
357	357	352	$17^X\mathrm{O'_{Cu}}-1^X\mathrm{Cu}-2^X\mathrm{O_{Cu}}$
596	596	596	$16^X\mathrm{O_{Cu}}-4^X\mathrm{Cu}+1^X\mathrm{O'_{Cu}}$
			B_{3g}
79	89	95	$(5^Y\mathrm{Ba}+4^Y\mathrm{O_{Ba}})+(3^Y\mathrm{Cu}+2^Y\mathrm{O_{Cu}}+3^Y\mathrm{O'_{Cu}})$
104	101	113	$(2^Y\mathrm{Ba}+1^Y\mathrm{O_{Ba}})-(7^Y\mathrm{Cu}+3^Y\mathrm{O_{Cu}}+7^Y\mathrm{O'_{Cu}})$
310	310	290	$17^Y\mathrm{O_{Ba}}-1^Y\mathrm{Ba}-1^Y\mathrm{O_{Cu}}$
361	361	382	$17^Y\mathrm{O_{Cu}}-1^Y\mathrm{Cu}+1^Y\mathrm{O_{Ba}}-2^Y\mathrm{O'_{Cu}}$
575	575	512	$16^Y\mathrm{O'_{Cu}}-4^Y\mathrm{Cu}+1^Y\mathrm{O_{Cu}}$
			B_{1u}
121	124	120	$6^Z\mathrm{Y}-(4^Z\mathrm{Ba}-1^Z\mathrm{O_{Ba}})-2^Z\mathrm{O_{Cu1}}+(4^Z\mathrm{Cu}+2^Z\mathrm{O_{Cu}}+2^Z\mathrm{O'_{Cu}})$
139	129	237	$7^Z\mathrm{Y}+(1^Z\mathrm{Ba}-5^Z\mathrm{O_{Ba}})+(5^Z\mathrm{Cu1}+2^Z\mathrm{O_{Cu1}})+(5^Z\mathrm{Cu}-3^Z\mathrm{O_{Cu}}-3^Z\mathrm{O'_{Cu}})$
227	228	239	$2^Z\mathrm{Y}-(1^Z\mathrm{Ba}-6^Z\mathrm{O_{Ba}})+(8^Z\mathrm{Cu1}+7^Z\mathrm{O_{Cu1}})-(5^Z\mathrm{Cu}+2^Z\mathrm{O_{Cu}}+1^Z\mathrm{O'_{Cu}})$
264	264	265	$13^Z\mathrm{O_{Cu}}-12^Z\mathrm{O'_{Cu}}$
295	294	270	$11^Z\mathrm{O_{Cu}}+11^Z\mathrm{O'_{Cu}}-4^Z\mathrm{Y}-1^Z\mathrm{Ba}+1^Z\mathrm{Cu1}-2^Z\mathrm{Cu}+1^Z\mathrm{O_{Ba}}$
336	336	372	$24^Z\mathrm{O_{Cu1}}-1^Z\mathrm{Ba}-3^Z\mathrm{Cu1}+1^Z\mathrm{Cu}-3^Z\mathrm{O_{Ba}}$
620	620	619	$15^Z\mathrm{O_{Ba}}-7^Z\mathrm{Cu1}-1^Z\mathrm{Cu}+1^Z\mathrm{O_{Cu1}}$
			B_{3u}
64	38	114	$5^X\mathrm{Y}-(3^X\mathrm{Ba}+3^X\mathrm{O_{Ba}})-(4^X\mathrm{Cu1}+3^X\mathrm{O_{Cu1}})+(5^X\mathrm{Cu}+5^X\mathrm{O_{Cu}}+4^X\mathrm{O'_{Cu}})$
126	126	117	$(2^X\mathrm{Ba}+3^X\mathrm{O_{Ba}})-(11^X\mathrm{Cu1}-4^X\mathrm{O_{Cu1}})-(1^X\mathrm{Cu}+1^X\mathrm{O_{Cu}})$
153	153	125	$8^X\mathrm{Y}-(5^X\mathrm{Cu}+5^X\mathrm{O_{Cu}}-2^X\mathrm{O'_{Cu}})-1^X\mathrm{Ba}$
212	212	215	$24^X\mathrm{O_{Cu1}}-1^X\mathrm{Ba}-4^X\mathrm{O_{Ba}}$
262	262	248	$16^X\mathrm{O_{Ba}}-2^X\mathrm{Ba}-1^X\mathrm{O'_{Cu}}+4^X\mathrm{O_{Cu1}}$
371	371	367	$17^X\mathrm{O'_{Cu}}-3^X\mathrm{Y}-1^X\mathrm{Cu}-2^X\mathrm{O_{Cu}}$
596	596	596	$16^X\mathrm{O_{Cu}}-4^X\mathrm{Cu}+1^X\mathrm{O'_{Cu}}$
			B_{2u}
65	40	104	$5^Y\mathrm{Y}-(3^Y\mathrm{Ba}+3^Y\mathrm{O_{Ba}})-(4^Y\mathrm{Cu1}+4^Y\mathrm{O_{Cu1}})+(5^Y\mathrm{Cu}+4^Y\mathrm{O_{Cu}}+5^Y\mathrm{O'_{Cu}})$
153	154	270	$4^Y\mathrm{Y}+(3^Y\mathrm{Ba}-1^Y\mathrm{O_{Ba}})-(8^Y\mathrm{Cu1}+8^Y\mathrm{O_{Cu1}})-(3^Y\mathrm{Cu}-2^Y\mathrm{O_{Cu}}+3^Y\mathrm{O'_{Cu}})$
156	155	283	$7^Y\mathrm{Y}-2^Y\mathrm{Ba}+(5^Y\mathrm{Cu1}+6^Y\mathrm{O_{Cu1}})-(4^Y\mathrm{Cu}-2^Y\mathrm{O_{Cu}}+4^Y\mathrm{O'_{Cu}})$
315	315	331	$17^Y\mathrm{O_{Ba}}-1^Y\mathrm{Ba}-2^Y\mathrm{Cu1}-1^Y\mathrm{O_{Cu}}-3^Y\mathrm{O_{Cu1}}$
375	375	348	$17^Y\mathrm{O_{Cu}}-3^Y\mathrm{Y}+1^Y\mathrm{Cu}-2^Y\mathrm{O'_{Cu}}$
575	575	512	$16^Y\mathrm{O'_{Cu}}-4^Y\mathrm{Cu}+1^Y\mathrm{O_{Cu}}$
593	593	525	$22^Y\mathrm{O_{Cu1}}-6^Y\mathrm{Cu1}+1^Y\mathrm{O_{Ba}}$

and within the three doublets (B_{3g},B_{2u}). At the same time, the splitting magnitude is rather large for the three doublets (A_g,B_{1u}). This gives evidence in favor of a different influence of interlayer interactions on modes with different symmetries.

When comparing the above theory with experiments, we emphasize the following results. The anomalous temperature behaviors at $T < T_c$ of the vibrations at 335 and 435 cm^{-1} in Raman spectra[27,28] as well as the vibrations at 275 and 315 cm^{-1} in ir spectra of $YBa_2Cu_3O_{7-\delta}$ ($\delta \rightarrow 0$)[29] confirm that all these modes are induced by vibrations of the same oxygen atoms, namely of the O_{Cu} and O'_{Cu} atoms [corresponding frequencies calculated are 335 and 439 cm^{-1} (A_g), 264 and 295 cm^{-1} (B_{1u})]. So, these even and odd vibrations do form the doublets.

D. The dispersion of vibrational branches

Within the framework of the dynamical model used, the dispersion curves of vibrational branches have also been calculated along symmetry lines in the BZ. Those for directions $(0,0,\xi)$ and $(0,\xi,0)$ are given in Fig. 2. The vibration symmetries at the Γ, Z, and Y points of the BZ were obtained in Sec. III.

It follows from Fig. 2 and from Table VI that all high-frequency branches corresponding to intralayer vibrations appear to be practically flat for the $(0,0,\xi)$ direction. This agrees with the predictions of the group-theory analysis above. At the same time, most of these phonon branches are essentially curved for the $(0,\xi,0)$ direction. Most vibrations from the low-frequency region (interlayer modes) manifest significant wave-vector dependence for all directions.

Note, the described behavior of the dispersion curves is an inherent property of the different perovskitelike compounds. It has been observed in inelastic neutron-scattering experiments for $YBa_2Cu_3O_7$,[30] La_2CuO_4,[31] and Nd_2CuO_4.[32] Thus, when classifying normal modes into intralayer and interlayer modes, one should take into account the following criteria: the character of mode displacement patterns, the dispersion of phonon branches, and the splitting of some normal modes.

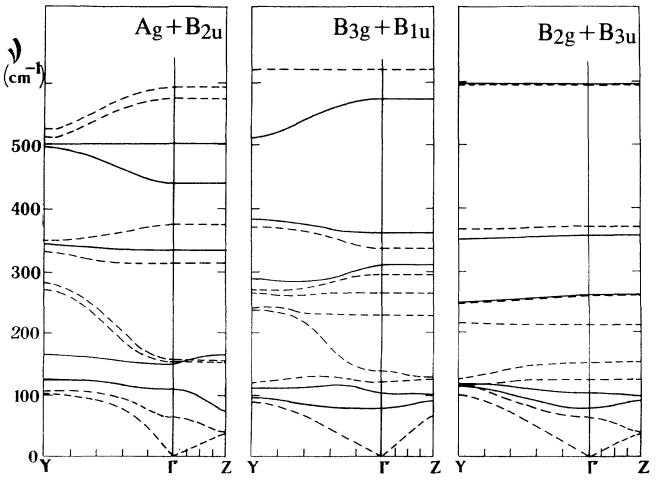

FIG. 2. Calculated dispersion curves corresponding at the BZ center to even (solid lines) and odd (dashed lines) modes in $YBa_2Cu_3O_7$ along the $(0,\xi,0)$, and $(0,0,\xi)$ symmetry lines.

V. RAMAN SPECTRA OF HTSC-COMPOUNDS

In this paper, we bring together the data on Raman spectra of Y-, Bi-, and Tl-based compounds. According to the interpretation of polarized Raman spectra of various perovskitelike superconductors, the most intense lines are induced by the phonons with A_{1g} (A_g) or B_{1g} symmetries. These modes are formed by displacements of atoms in the z direction. Table VII and Fig. 3 show the experimental frequency values of these vibrations in Y-, Tl-, and Bi-based superconductors.[1,6–8,10,33–39]

Raman-active E_g modes (tetragonal structures) as well as the B_{2g} and B_{3g} modes (orthorhombic structures) are formed by displacements of atoms in the x and y directions. The corresponding lines in the Raman spectra are weak. For example, in 1:2:3- compounds these lines are 100 times weaker than the A_g lines.[40] In the Tl- and some Bi-based compounds, these modes have not been observed.

One can see that it is possible to divide the Raman spectra into low- and high-frequency regions. The lines from the low-frequency region ($\nu \leq 200$ cm^{-1}) can be attributed to interlayer vibrations participated in by both the heavy atoms (Bi, Tl, Cu, Ba, Sr) and the O atoms.

The intralayer vibrations are observed in the high-frequency region. The latter region may also be subdivided into a set of spectral subregions. The vibrations of O_{Cu} atoms lie in the intermediate subregion (250–450 cm^{-1}). The out-of-phase B_{1g} (A_g) vibrations have a lower frequency and the in-phase A_{1g} (A_g) vibrations

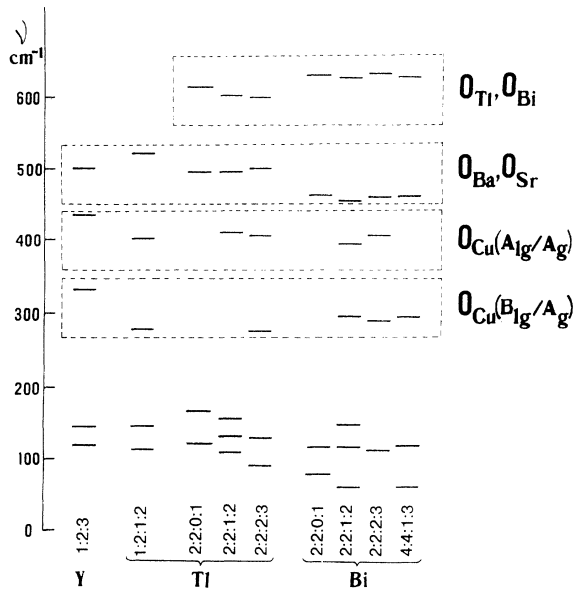

FIG. 3. Frequencies of A_{1g} (A_g) and B_{1g} (A_g) modes in $YBa_2Cu_3O_7$ (Ref. 33), Tl-1:2:1:2 (Refs. 34,35), Tl-2:2:0:1 (Ref. 36), Tl-2:2:1:2 (Ref. 39), Tl-2:2:2:3 (Ref. 37), Bi-2:2:0:1 (Ref. 20), Bi-2:2:1:2 (Ref. 38), Bi-2:2:2:3 (Ref. 1), Bi-4:4:1:3 (Ref. 10).

TABLE VII. Raman line frequencies and their assignments.

		Frequencies (cm^{-1}), assignment, symmetry							
Compound	Ref.	Bi A_{1g}, A_g	Tl A_{1g}	Ba,Sr A_{1g}, A_g	Cu A_{1g}, A_g	O_{Cu} B_{1g}, A_g	O_{Cu} A_{1g}, A_g	$O_{Ba,Sr}$ A_{1g}, A_g	$O_{Tl,Bi}$ A_{1g}, A_g
Y-1:2:3	6			117	148	335	438	502	
Y-1:2:3	7			119	145	336	435	499	
Y-1:2:3	33			118	145	335	440	500	
Tl-1:2:1:2	34			116	146		403	520	
Tl-1:2:1:2	35			120	148	278		525	
Tl-2:2:0:1	36		167	122				495	612
Tl-2:2:1:2	39		130	108	158	316	407	494	599
Tl-2:2:1:2	34		132	109	158		410	495	602
Tl-2:2:2:3	37		129	92		275	405	498	599
Bi-2:1:0:0	8	83							651
Bi-2:2:0:1	20	80		118				461	629
Bi-2:2:1:2	38	62		118	148	296	395	456	626
Bi-2:2:2:3	1			115		290	406	460	633
Bi-4:4:1:3	10	63		120		295		461	627

have a higher frequency.

In the higher-frequency subregion of the Raman spectra (450–520 cm^{-1}), there are A_{1g} (A_g) vibrations of O_{Ba} atoms in Y- and Tl-based superconductors, and of O_{Sr} atoms in Bi-based compounds. These are so-called bridge oxygen atoms connecting two Cu atoms, or Cu and Tl, or Cu and Bi in the corresponding systems. Finally, the highest-frequency A_{1g} (A_g) modes (600–650 cm^{-1}) involve the vibrations of O_{Tl} and O_{Bi} atoms.

It is clearly seen that the frequencies of the intralayer vibrations of oxygen atoms belonging to a particular layer vary insignificantly for crystals not only within the Bi-based superconductor family[1] but also within the entire group of compounds under consideration (i.e., for Y-, Tl-, and Bi-based families). Therefore, these frequencies can be considered to be the signatures of each layer.

VI. QUASI-2D BEHAVIOR OF THE PHONON SUBSYSTEMS OF PEROVSKITELIKE SUPERCONDUCTORS

Now, let us summarize the main characteristics of the phonon subsystems of perovskitelike superconductors, following from the layered structure of these materials. To perform a group-theory analysis of normal vibrations (Sec. III), we considered isolated layers, determined the symmetry of acoustic and optical layer modes, and established a correspondence between layer and bulk vibrations. As a result, two important conclusions have been made. First, some intralayer modes split into Raman-active and ir-active components and, second, the intralayer modes are nearly dispersionless along the Γ-Z symmetry line in the BZ.

On the other hand, the lattice dynamical model of $YBa_2Cu_3O_7$ was chosen without an *a priori* assumption of a layered character of the structure. Nevertheless, the results of lattice dynamical calculations (Sec. IV) completely confirmed the group-theory predictions. What is more important, both the conclusions of the group-theory analysis and the results of lattice dynamical calculations are confirmed by experiments on inelastic neutron scattering as well as by optical measurements. Thus, the validity of both the layer approach and the chosen separation of perovskitelike crystal lattices into single layers has been justified.

Another significant result is the small variation of intralayer phonon frequencies when passing from one compound to another within the Y-, Tl-, and Bi-based compounds considered (Sec. V).

Summing up, the conclusion can be made that the layered structure of the perovskitelike compounds is responsible for the principal characteristics of their phonon subsystems, and that the phonon subsystems manifest quasi-2D behavior.

VII. SANDWICH CONCEPTION OF HIGH-TEMPERATURE SUPERCONDUCTIVITY

The strong anisotropy of the high-T_c superconductors manifests itself in their transport, elastic, and optical properties. To comprehend better the special features of these compounds, one should consider the idea of perovskitelike superconductors as compounds with quasi-2D properties. The structure of cuprate superconductors can be considered as a set of conducting CuO_2 layers "sandwiched" by block layers.[11]

The above analysis shows the phonon subsystem to have quasi-2D character. Weak coupling between the conducting CuO_2 layers leads to quasi-2D behavior of the electron subsystem too. This manifests itself particularly in the 2D character of the electron bands found by band numerical calculations (see, e.g., Refs. 19,41).

Since the thickness of the blocking-layer stacks separating the adjacent CuO_2 layers does not exceed 10–20 Å, the sandwich conception of Ref. 42 is applicable. This conception has been widely discussed with respect to layered superconductors.[43] It supposes the conducting layers to be separated by insulating regions.

In this case, phonons and electron excitations in the blocking-layer stack may play the role of coupling bosons.

The correlation[44,45] between the critical temperature T_c and frequencies of intense Raman lines in perovskite-like superconductors seems to be a pronounced manifestation of the importance of nonpolar phonons in the high-T_c superconductivity mechanism. The essence of this correlation is the regular increases both in T_c and in the characteristic Raman frequencies within the row La-$\rightarrow$Y-$\rightarrow$Bi-$\rightarrow$Tl-based superconductors. We emphasize that the highest-frequency intense lines in the Raman spectra are caused by the A_{1g} (A_g) vibrations of oxygen atoms in the layers separating copper oxide planes (see Sec. V). Indeed, this vibration is related to oxygen atoms in the LaO layers in La-based compounds, in the BaO layers in $YBa_2Cu_3O_7$, and in the BiO (TlO) layers in Bi (Tl) compounds.

We believe that the correlation is not accidental and that it reflects a common proportionality between T_c and an average frequency describing the whole vibrational spectrum.[43,46,47] The correlation was explained in Refs. 48,49. In Ref. 48, the transition temperature T_c was calculated within the framework of the Eliashberg theory,[50] the frequencies of nonpolar (Raman-active) phonons being taken as a basis. The main result of Ref. 48 consists in a good agreement between experimental and calculated T_c for all superconductor families at the same $\lambda \simeq 1.5-2$ and $\mu^* \simeq 0.1-0.2$.

Such a value of the coupling constant λ is reasonable. Indeed, there are a number of estimations of λ. The analysis of results of very different experiments gives $\lambda \simeq 1-3$. According to tunneling experiments, $\lambda \simeq 2.04$,[51] $\lambda \simeq 3.5$.[52] Measurements on the electronic specific heat give $\lambda \simeq 2$.[53] To describe the ir properties of high-T_c superconductors, the electron-boson coupling constant λ was supposed to be close to 2 in Ref. 54. According to the results of electron-spin resonance investigations, the parameter λ is 1.65.[55] From the resistivity data on single crystals together with results of optical investigations, λ was estimated to be about 1.5–2 in Ref. 56.

The correlation between T_c and Raman frequencies[44,45] seems to be a result of a common superconductivity mechanism for all high-T_c superconductors. This arises from the presence of the same CuO_2 layers (which determine the properties of the quasi-2D electron subsystem) and from the dissimilarity of the separating layers (which determine important properties of the quasi-2D phonon subsystem).

An advantage of sandwich systems is the possibility of the selection of layers with the most favorable properties. Thus, the electron and phonon subsystems can be optimized practically independently.[43] The idea of such an optimization relevant to high-T_c superconductors was formulated in Ref. 45. According to Ref. 45, the phonon subsystem determines the maximum value of the critical temperature within each high-T_c superconductor family. Within each of the families, $T_{c,\max}$ is realized in a compound with an optimized electron subsystem, in particular with the carrier density $n \simeq 10^{21}$ cm^{-3}.[45,57] The existence of such a maximum in the T_c vs n dependence can be explained within the framework of the phonon mechanism of superconductivity, if quasi-two-dimensionality of the electron subsystem is assumed.[58]

VIII. CONCLUSIONS

Paying special attention to the layered structure of the crystal lattices of high-T_c superconductors, we have analyzed step by step their crystal structures, phonon symmetry properties, vibrational spectra, and the role of phonons in the superconductivity mechanism. As a result, the quasi-2D nature of the phonon subsystem of perovskitelike superconductors has been established. The differentiation of roles of the various layers in creating the high-T_c superconductivity phenomenon has been discussed.

ACKNOWLEDGMENTS

This work was supported by the Scientific Council on HTSC problems, Grant No. 91084 "ELPHON" of the Russian State program "High-temperature superconductivity."

[1]A. A. Bush, I. N. Goncharuk, Yu. E. Kitaev, M. F. Limonov, Yu. F. Markov, and R. A. Evarestov, Zh. Eksp. Teor. Fiz. **102**, 1587 (1992) [Sov. Phys.–JETP **75**, 857 (1992)].

[2]R. Zallen, M. L. Slade, and A. T. Ward, Phys. Rev. B **3**, 4257 (1971).

[3]I. P. Ipatova, Yu. E. Kitaev, V. G. Malyshkin, and R. A. Evarestov, Fiz. Tverd. Tela (Leningrad) **32**, 1565 (1990) [Sov. Phys.–Solid State **32**, 918 (1992)].

[4]R. A. Evarestov and V. P. Smirnov, in *Site Symmetry in Crystals: Theory and Applications*, edited by M. Cardona, Springer Series in Solid State Sciences Vol. 108, (Springer, Heidelberg, 1993).

[5]R. Liu, C. Thomsen, W. Kress, M. Cardona, B. Gegenheimer, F. W. de Wette, J. Prade, A. D. Kulkarni, and U. Schroder, Phys. Rev. B **37**, 7971 (1988).

[6]V. D. Kulakovskii, O. V. Misochko, and V. B. Timofeev, Fiz. Tverd. Tela (Leningrad) **31**, 220 (1989) [Sov. Phys.–Solid State **31**, 1599 (1989)].

[7]M. F. Limonov, Yu. F. Markov, A. G. Panfilov, B. S. Razbirin, P. P. Syrnikov, and A. A. Bush, Physica C **191**, 255 (1992).

[8]A. A. Bush, Yu. E. Kitaev, M. A. Kulikov, M. F. Limonov, Yu. F. Markov, A. A. Novikov, V. P. Sirotinkin, Yu. V. Titov, and R. A. Evarestov, Fiz. Tverd. Tela (Leningrad) **34**, 148 (1992) [Sov. Phys.–Solid State **34**, 77 (1992)].

[9]A. A. Bush, B. N. Romanov, I. V. Isakov, V. A. Sarin, S. A. Ivanov, and V. V. Zhurov, Sverkhprovodimost: Fiz. Khim. Tekh. **5**, 364 (1992).

[10]A. A. Bush, I. N. Goncharuk, Yu. E. Kitaev, M. F. Limonov, Yu. F. Markov, and R. A. Evarestov, Fiz. Tverd. Tela (Leningrad) **34**, 2178 (1992) [Sov. Phys.–Solid State **34**, 1164 (1992)].

[11]Y. Tokura, Physica C **185-189**, 174 (1991).

[12]O. V. Kovalev, Fiz. Tverd. Tela (Leningrad) **17**, 1700 (1975) [Sov. Phys.–Solid State, **17**, 1106 (1975)].

[13]D. L. Rousseau, R. P. Bauman, and S. P. S. Porto, J. Raman Spectrosc. **10**, 253 (1981).
[14]E. A. Wood, Bell System Monograph No. 4680 (1964).
[15]S. C. Miller and W. F. Love, *Tables of Irreducible Representations of Space Groups and Corepresentations in Magnetic Space Groups* (Pruett, Boulder, 1967).
[16]C. J. Bradley and A. P. Cracknell, *The Mathematical Theory of Symmetry in Solids* (Clarendon, Oxford, 1972).
[17]*International Tables for Crystallography, Vol. A. Space Group Symmetry,* edited by T. Hahn (Reidel, Dordrecht, 1983).
[18]Yu. E. Kitaev and R. A. Evarestov, Fiz. Tverd. Tela (Leningrad) **31**, 76 (1989) [Sov. Phys.–Solid State **31**, 958 (1989)].
[19]V. A. Veryazov, Yu. E. Kitaev, V. P. Smirnov, and R. A. Evarestov, in *High-T_c Superconductivity. Fundamental and Applied Studies,* edited by A. A. Kiselev (Mashinostroeniye, Leningrad, 1990), Vol. 1, p. 446 (in Russian).
[20]A. A. Bush, Yu. E. Kitaev, M. F. Limonov, Yu. F. Markov, A. A. Novikov, and R. A. Evarestov, Physica C **190**, 477 (1992).
[21]L. A. Chernozatonskii, Pis'ma Zh. Eksp. Teor. Fiz. **49**, 280 (1989) [JETP Lett. **49**, 319 (1989)].
[22]M. F. Limonov and A. P. Mirgorodsky (unpublished).
[23]M. B. Smirnov, Opt. Spektrosk. **65**, 311 (1988) [Opt. Spectrosc. **65**, 186 (1988)].
[24]V. N. Molchanov, L. A. Muradyan, and V. I. Simonov, Pis'ma Zh. Eksp. Teor. Fiz. **49**, 222 (1989) [JETP Lett. **49**, 257 (1989)].
[25]A. V. Bazhenov and V. B. Timofeev, Sverkhprovodimost: Fiz. Khim. Tekh. **3**, 1174 (1990) [Supercond. Phys. Chem. Technol. **3**, S27 (1992)].
[26]J. D. Jorgensen, S. Pei, P. Lightfoot, D. G. Hinks, B. W. Veal, B. Dabrowski, A. P. Paulikas, and R. Kleb, Physica C **171**, 93 (1990).
[27]R. M. Macfarlane, H. Rosen, and H. Seki, Solid State Commun. **63**, 831 (1987).
[28]C. Thomsen, M. Cardona, B. Friedl, C. O. Rodriguez, I. I. Mazin, and O. K. Andersen, Solid State Commun. **75**, 219 (1990).
[29]A. Wittlin, R. Liu, M. Cardona, L. Genzel, W. Konig, W. Bauhofer, Hj. Mattausch, A. Simon, and F. Garcia-Alvarado, Solid State Commun. **64**, 477 (1987).
[30]W. Reichardt, N. Pyka, L. Pintschovius, B. Hennion, and G. Collin, Physica C **162–164**, 464 (1989).
[31]H. Rietschel, L. Pintschovius, and W. Reichardt, Physica C **162–164**, 1705 (1989).
[32]L. Pintschovius, N. Pyka, W. Reichardt, A. Yu. Ruminatsev, N. L. Mitrofanov, A. S. Ivanov, G. Gollin, and P. Bourges, Physica C **185–189**, 156 (1989).
[33]R. Feile, Physica C **159**, 1 (1989).
[34]L. V. Gasparov, V. D. Kulakovkii, O. V. Misochko, V. B. Timofeev, N. N. Kolesnikov, and M. P. Kulakov, Pis'ma Zh. Eksp. Teor. Fiz. **49**, 58 (1989) [JETP Lett. **49**, 68 (1989)].
[35]K. F. McCarty, D. S. Ginley, D. R. Boehme, R. J. Baughman, E. L. Venturini, and B. Morosin, Physica C **156**, 119 (1988).
[36]V. B. Timofeev, A. A. Maksimov, O. V. Misochko, and I. I. Tartakovskii, Physica C **162–164**, 1409 (1989).
[37]K. F. McCarty, D. S. Ginley, D. R. Boehme, R. J. Baughman, and B. Morosin, Solid State Commun. **68**, 77 (1988).
[38]A. A. Bush, I. V. Gladyshev, A. A. Golub, O. Yu. Mashtakov, V. Yu. Mirovitskii, M. F. Limonov, Yu. F. Markov, and A. G. Panfilov, Sverkhprovodimost: Fiz. Khim. Tekh. **2**, 104 (1989).
[39]C. Thomsen, in *Light Scattering in Solids VI,* edited by M. Cardona and G. Guntherodt, Topics in Applied Physics Vol. 68 (Springer, Berlin, 1991), p. 285.
[40]K. F. McCarty, J. Z. Liu, R. N. Shelton, H. B. Radousky, Phys. Rev. B **41**, 8792 (1990).
[41]W. E. Pickett, Rev. Mod. Phys. **61**, 433 (1989).
[42]V. L. Ginzburg, Zh. Eksp. Teor. Fiz. **47**, 2318 (1964); Phys. Lett. **13**, 101 (1964).
[43]*High Temperature Superconductivity,* edited by V. L. Ginzburg and D. A. Kirzhnits (Consultants Bureau, New York, 1982).
[44]M. F. Limonov, Yu. F. Markov, A. G. Panfilov, B. S. Razbirin, A. A. Bush, and I. S. Dubenko, Solid State Commun. **75**, 511 (1990).
[45]M. F. Limonov, Yu. F. Markov, A. G. Panfilov, and B. S. Razbirin, Sverkhprovodimost: Fiz. Khim. Tekh. **4**, 233 (1991) [Supercond. Phys. Chem. Technol. **4**, 198 (1991)].
[46]W. L. McMillan, Phys. Rev. **167**, 331 (1968).
[47]P. B. Allen and R. C. Dynes, Phys. Rev. B **12**, 905 (1975).
[48]M. F. Limonov and A. G. Panfilov, Sverkhprovodimost: Fiz. Khim. Tekh. **5**, 1342 (1992).
[49]E. A. Pashitskii, Sverkhprovodimost: Fiz. Khim. Tekh. **3**, 2669 (1990) [Supercond. Phys. Chem. Technol. **3**, 1867 (1990)].
[50]G. M. Eliashberg, Zh. Eksp. Teor. Fiz. **38**, 966 (1960).
[51]R. S. Gonelly, L. N. Bulayevskii, O. V. Dolgov, and S. I. Vedeneev, in Proceedings of the Congresso SATT 3 (World Scientific, Singapore, 1991).
[52]P. Samuely, S. I. Vedeneev, S. V. Meshkov, G. M. Eliashberg, A. G. M. Jansen, and P. Wyder, in *Proceedings of the 1st International Conference on Point-Contact Spectroscopy, Kharkov, 1991* [Sov. J. Low Temp. Phys. **18**, 567 (1991)].
[53]S. V. Shulga, O. V. Dolgov, and I. I. Mazin, Physica C **192**, 41 (1992).
[54]S. V. Shulga, O. V. Dolgov, and E. G. Maksimov, Physica C **178**, 266 (1991).
[55]G. B. Teitel'baum, Yu. S. Greznev, V. E. Kataev, and E. F. Kukovitsky, Physica C **185–189**, 1209 (1991).
[56]I. I. Mazin and O. V. Dolgov, Phys. Rev. B **45**, 2509 (1992).
[57]A. I. Golovashkin, Usp. Fiz. Nauk **152**, 553 (1987).
[58]V. Z. Kresin and H. Moravitz, Solid State Commun. **74**, 1203 (1990).